Analytical Methods in Environmental Chemistry Journal Vol 2 (2019) 67-78

AMECJ

Research Article, Issue 3

Analytical Methods in Environmental Chemistry Journal

Journal home page: www.amecj.com/ir

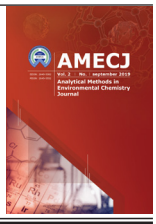

A novel sorbent based on metal–organic framework for mercury separation from human serum samples by ultrasound assisted- ionic liquid-solid phase microextraction

Negar Motakef-Kazemi[a,*]

[a,*] *Department of Medical Nanotechnology, Faculty of Advanced Sciences and Technology, Tehran Medical Sciences, Islamic Azad University, Tehran, Iran.*

ARTICLE INFO:

Received 14 Jul 2019

Revised form 19 Aug 2019

Accepted 30 Aug 2019

Available online 30 Sep 2019

Keywords:

Metal–organic framework;

Ultrasound assisted -micro-solid phase extraction;

Mercury;

Serum samples;

Cold vapor atomic absorption spectrometry

ABSTRACT

In this research, the metal–organic framework (MOF) as a solid phase was used for separation mercury [Hg (II)] inhuman serum sample by ultrasound assisted- Ionic Liquid-solid phase microextraction procedure (USA- IL-µ-SPE). Mercury extracted from serum sample by $[Zn_2(BDC)_2(DABCO)]_n$ as MOF at pH=8. Hydrophobic ionic liquid ([BMIM] [PF6]) was used as solvent trap for Hg-MOF-NC from the sample solution. The phase of Hg-MOF-NC was back extracted by 0.5 mL of HNO_3 (0.2 mol L-1) and finally mercury concentration determined with cold vapor-atomic absorption spectrometry (CV-AAS) after dilution with 0.5 mL of DW. Under the optimal conditions, the linear range, limit of detection and preconcentration factor were obtained 0.02–5.5 µg L^{-1}, 6.5 ng L^{-1} and 9.8 for serum samples, respectively (%RSD<5%). The validation of methodology was confirmed by standard reference materials (SRM).

1. Introduction

Today, metal-organic frameworks have received considerable attention as porous coordination polymers (PCPs) and porous hybrid organic–inorganic materials because of their unique properties [1-2]. MOFs can be synthesized via self-assembly of metal ions (or metal clusters) as metal centers, and bridging ligands as linkers [3-4]. In recent years, MOFs wildly have been studied for their potential applications in many areas such as gas storage [5], separation [6], catalysis [7], optics [8], photonic [9], ion exchange [10], molecular array [11], biomedicine [12], sensing [13], drug delivery [14], luminescent [13, 15], magnetic [16], and semiconductors [17]. Several methods have been proposed to remove hazardous materials from water such as electrochemical [18], chemical coagulation [19], reverse osmosis membrane [20], and adsorbent [21-23]. The absorbent materials have been studied for different species such as nitrobenzene [24-26], phenol [27], p-xylene hydrocarbon [28], dye [29-32], heavy metal [33-34], humic acid [35], and nitrate [36-37] from the waste water. Mercury is a chemical element and heavy metal with very toxic effect. This non-essential metal can be distributed

* Corresponding author: Negar Motakef-Kazemi

Email: motakef@iaups.ac.ir

https://doi.org/10.24200/amecj.v2.i03.68

in the environment, natural products, and human body [38-39]. The exposure to high mercury can be resulted to the changes in the central nervous system, irritability, fatigue, behavioral changes, tremors, headaches, hearing and cognitive loss, dysarthria, incoordination, and hallucinations [40]. Mercury compounds can be harmed the liver and kidneys, resulting some disorder in enzyme activity, illness, and death [41-42]. Recently, the applications of mercury adsorbents are expanded due to increased level and toxic effect [43-44]. In present study, $Zn_2(BDC)_2(DABCO)$ MOF was synthesized by solvothermal method for mercury absorption from serum and standard solution with CV-AAS by USA- IL-μ-SPE procedure. The 1-octyl-3-methylimidazolium hexafluorophosphate ([OMIM][PF_6]) as a hydrophobic ionic liquid was used for separating of Hg-MOFfrom liquid phase. The proposed method was validated by spike of real samples and CRM (NIST).

2. Experimental

2.1. Reagents and Materials

All reagents with high purity and analytical grade were purchased from Merck (Darmstadt, Germany), unless otherwise stated. Materials including zinc acetate ehydrate ($Zn(Oac)_2.2H_2O$), 1,4 benzenedicarboxylic acid (BDC), 1,4-diazabicyclo [2.2.2] octane (DABCO), dimethylformamide (DMF) were used for synthesis of $Zn_2(BDC)_2(DABCO)$ MOF. All aqueous solutions were prepared in ultra-pure deionized water (R≥18 MΩ cm^{-1}) from Milli-Q plus water purification system (Millipore, Bedford, MA, USA). An Hg (II) standard stock solution (1000 mg L^{-1} in 1% nitric acid, 250 mL) was purchased from Fluka, Buchs, Switzerland. The experimental and working standard solutions were prepared daily by diluting the stock solutions with deionized water. The solutions were freshly prepared and stored just in a fridge (4 °C) to prevent decomposition. A 0.6% (w/v) sodium borohydride reagent solution was prepared daily by dissolving an appropriate amount of $NaBH_4$ in 0.5% (w/v) sodium hydroxide and used as a reducing agent. 1-butyl-3-methylimidazolium hexafluorophosphate [HMIM][PF6] was obtained from Sigma–Aldrich (M) Sdn. Bhd., Malaysia. The pH adjustments of samples were made using nitric acid (0.1 mol L^{-1}) for pH 1-2, and appropriate buffer solutions including sodium acetate (CH_3COONa/CH_3COOH, 1-2 mol L^{-1}) for pH 3.75-5.75, sodium phosphate (Na_2HPO_4/NaH_2PO_4, 0.2 mol L^{-1}) for pH of 5.8-8.0, and ammonium chloride (NH_3/NH_4Cl, 0.2 mol L^{-1}) for pH 8-10. All the laboratory glassware and plastics were cleaned by soaking in nitric acid (10%, v/v) for at least 24 h and then rinsed with deionized water before use. Due to hazardous effects of Hg solutions, gloves, safety mask, and laboratory hood should be used when mercury standard solutions are prepared.

2.2. Characterization

The MOF was characterized by Fourier transform infrared spectroscopy (FTIR), powder X-ray diffraction (XRD), and scanning electron microscope (SEM). FTIR spectra were recorded on a Shimadzuir 460 spectrometer in a KBr matrix in the range of 400–4000 cm^{-1}. Powder X-ray diffraction pattern was performed for evaluation of crystalline structure of bismuth oxide NP using a Philips Company X'pert diffractometer utilizing Cu-Ka radiation (ASENWARE, AW-XBN300, China). Scanning electron microscope was investigated the morphology and MOF (KYKY, EM3200, China). Determination of mercury was performed with an atomic absorption spectrometer (GBC 932– HG3000-AUS, Australia) equipped with a flow injection cold vapor module (FI-CV-AAS), deuterium-lamp background corrector, Hg hollow-cathode lamp, and a circulating reaction loop. The working conditions of FI-CV-AAS were given in Table 1. The pH values of the solutions were measured by a digital pH meter (Metrohm, model 744, Herisau, Switzerland). A Hettich centrifuge (model EBA 20, Germany) and an ultrasonic bath with heating system (Tecno-GAZ SPA, Italy) were used throughout this study.

2.3. Synthesis of MOF

The $Zn_2(BDC)_2(DABCO)$ MOF was prepared via

Table 1. The FI-CV-AAS conditions for determination of mercury in standard samples.

Features	Value
Linear range, µg L^{-1}	0.2-55
Wavelength, nm	253.7
Lamp current, mA	3.0
Slit, nm	0.5
Mode	Peak area
HCl carrier solution 37%, mol L^{-1}	3.0
$NaBH_4$ reducing agent, % (m/v)	0.6 (in 0.5% w/v NaOH)
Argon flow rate, mL min^{-1}	10.0
Sample flow rate, mL min^{-1}	3.0
Reagent flow rate, mL min^{-1}	5.0

the self-assembly of primary building blocks. In a typical reaction, Zn $(OAc)_2.2H_2O$ (0.132 g, 2 mmol), BDC (0.1 g, 2 mmol), and DABCO (0.035 g, 1 mmol) were added to 25 ml DMF [3]. The reactants were sealed under reflux and stirred at 90 °C for 3 h. Then, the reaction mixture was cooled to room temperature, and filtered. The white crystals were washed with DMF to remove any metal and ligand remained, and dried in a vacuum. DMF was removed from white crystals with a vacuum furnace at 150 °C for 5 h.

2.4. General procedure of mercury adsorption

By USA-IL-µ-SPE procedure, 10 mL polytetrafluoroethylene (PTFE) centrifuge tube was used for this study. First, 10 mL of serum sample or standard aqueous solution containing Hg (II) with concentration in the range of 0.1-5.5 µg L^{-1} was adjusted to optimum pH of 8 with sodium phosphate buffer solution (Na_2HPO_4/ NaH_2PO_4, 0.2 mol L^{-1}) and transferred into the 10 mL PTFE centrifuge tube. Then 50 mg of [OMIM][PF6] dispersed in 100 µL acetone was mixed with 20 mg $Zn_2(BDC)_2(DABCO)$ as MOF sorbent and rapidly injected by a syringe into the serum/ standard solution. The resulting mixture was shaken in ultrasonic bath for 5 min at 25 ºC. Hg (II) was extracted and separation by MOF. The $[Zn_2(BDC)_2(DABCO)]_n$-Hg was trapped with IL and centrifuged at 4000×g for 3 min. The Hg-MOF /IL was settled down in bottom of the conical centrifuge tube and the aqueous phase was removed with a transfer pipette. Finally, mercury species retained on the sorbent were eluted by adding 0.5 mL of 0.3 molar HNO_3 and vigorously shaking the tube for 1 min. The eluent phase was separated by centrifuging of the remaining mixture and Hg (II) ions were analyzed by CV-AAS after dilution with deionized water up to 1 ml. Figure 1 was shown general procedure of mercury adsorption.

3. Results and Discussion

3.1. Fourier transforms infrared spectroscopy for MOF

The FTIR spectra of MOF were recorded in the range of 400–4000 cm-1 with KBr pellets by fourier transforms infrared spectroscopy (Fig. 2). The C–H aromatic band is shown at 3424 cm^{-1}. The aliphatic C–H asymmetric stretching is assigned at 2960 cm^{-1}. The peak at 2357 cm^{-1} is related to CO_2 which exist in environment. The C=O stretching and carboxylic group are assigned at 1587 cm^{-1} and 1387 cm^{-1} respectively. FTIR spectra corresponded to the reported results [1].

3.2. X-ray diffraction of MOF

The XRD measurement was used to determine the crystalline structure of MOF in 2θ range ۵° to ۳۰° (Fig. 3). The position and diffraction properties of the peaks are similar to the pattern of previously reported result [1].

3.3. Scanning electron microscopy for MOF

The size and morphology structures of samples

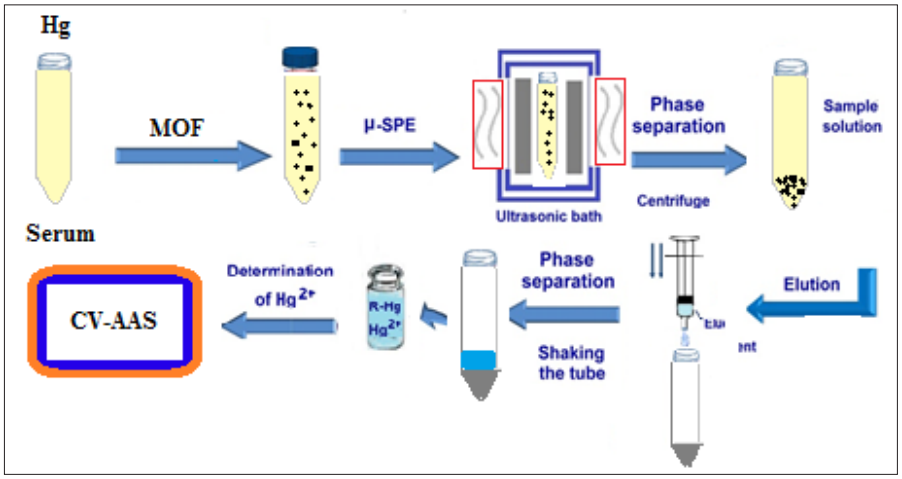

Fig. 1. General procedure of mercury adsorption based on MOF by USA-IL-μ-SPE

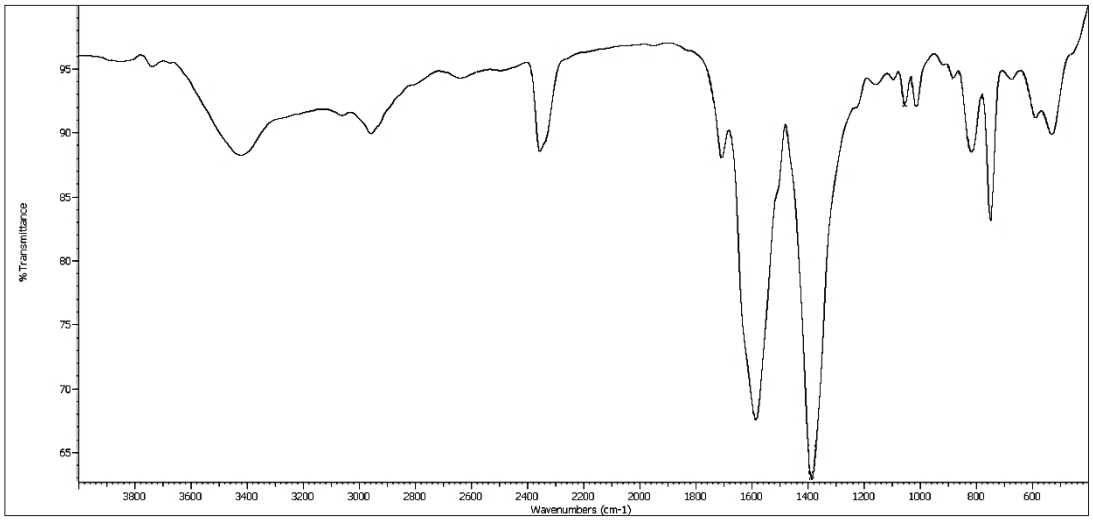

Fig. 2. FTIR spectra of $Zn_2(bdc)_2(dabco)$ MOF

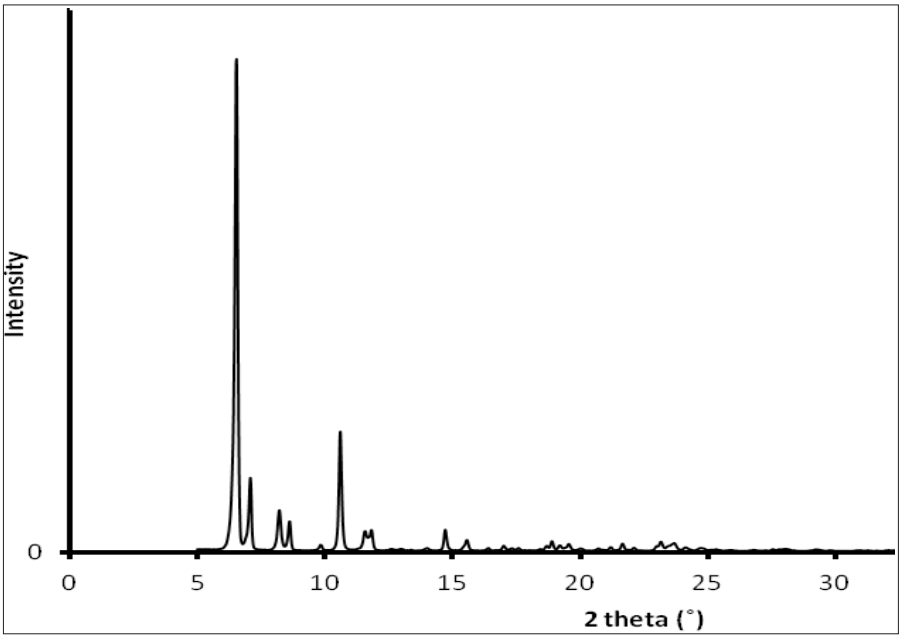

Fig. 3. XRD pattern of $Zn_2(bdc)_2(dabco)$ MOF

were studied using SEM that shown rod-shaped with an average diameter of 70 nm, and the length of 350 nm (Fig. 4).

3.4. Adsorption mechanism

The compounds of MOF $[Zn_2(bdc)_2(dabco)]_n$ such as, bdc (COO-) and dabco(N:) was used for chemical extraction of mercury from serum and standard solution samples at optimized pH. These ligands as a suitable material can be extracted the mercury ions in human biological sample at pH=8. The MOF are coordinating with the cations of Hg via nitrogen and carbocyclic bond which was deprotonated at basic pH. The mechanism of chemical and physical adsorption carried out by MOF at pH 7.5-8.5 for mercury in serum samples. The results showed us the recovery of physical adsorption in low pH without nitrogen covalence bonding (pH=3─6) was achieved 43.8 % and increased more than 95% by chemical bonding of MOF with Hg(MOF─N:→Hg) at pH=7.5─8.5 (Fig. 5)

3.5. The optimization

The optimization was investigated for the ultrasound-assisted ionic liquid-micro solid phase extraction conditions. The USA-IL-µSPE procedure provides novel and interesting approach using the MOF sorbent for extraction of mercury from water and serum samples. In order to obtain optimum speciation conditions and quantitative recoveries of inorganic and organic mercury species with good sensitivity and precision, the presented USA- IL-µSPE method was optimized for various analytical parameters. Moreover, in order to optimization of effecting parameters, standard solutions containing different concentrations of Hg (II) in the range of 0.1–5.5 µg L^{-1} were examined.

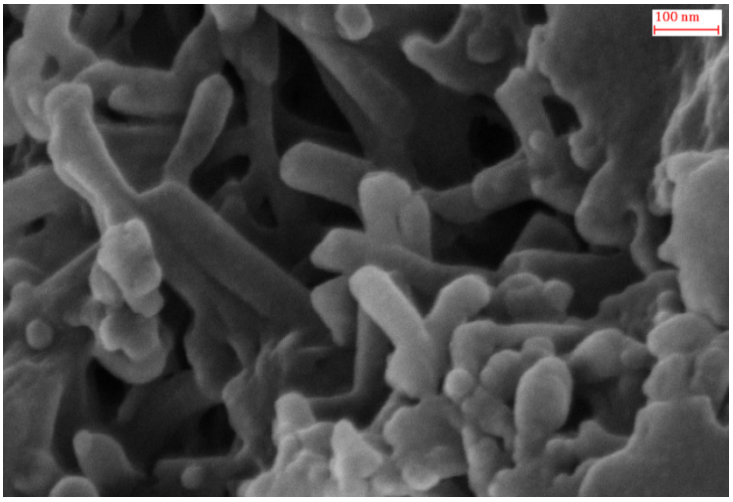

Fig. 4. SEM of $Zn_2(bdc)_2(dabco)$ MOF

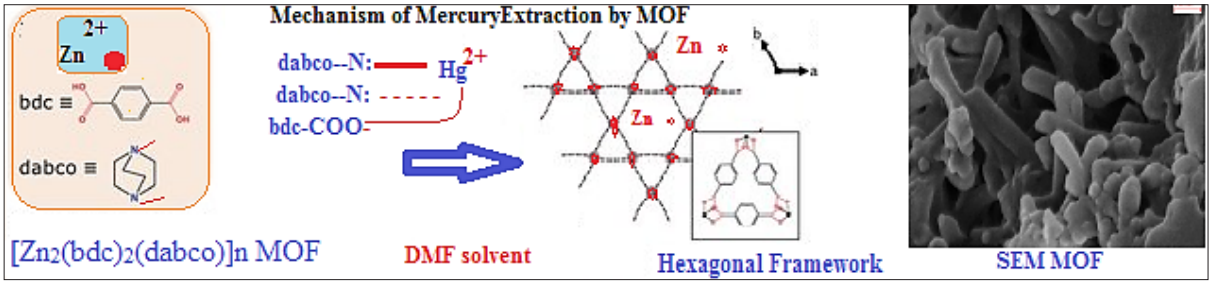

Fig. 5. The mechanism of mercury absorption by MOF

3.5.1. Back extraction of mercury from MOF

The recovery percentage was investigated for mercury absorption by MOF in presence of different acids such as HNO_3, HCl, H_2SO_4, and CH_3COOH (Fig. 6), and selected 0.3 molar HNO_3 as optimum.

3.5.2. The pH effect of MOF

The pH of the sample is an important role to high recovery and extraction of Hg in human serum matrixes. The effect of serum pH on the extraction of Hg(II) based on MOF has studied from pH of 2 to 11, containing 0.1-5.5 µg L^{-1} of standard Hg(II) by USA- IL-µ-SPE method. Based on Figure 7, the extraction of Hg ions in serum and standard solution samples were increased between pH from 7.5 to 8.5. The recovery of mercury extraction were achieved more than 95% in pH=8 and decreased at pH more than 8.5 and less than 7.5. Consequently, the pH of 8 was used in further study for Hg extraction from serum and standard solution samples. In addition, the extra extraction of mercury was achieved by increasing MOF mass but, some of essential metals (Cu, Zn, Ca, Mn, Mg,) may be removed from

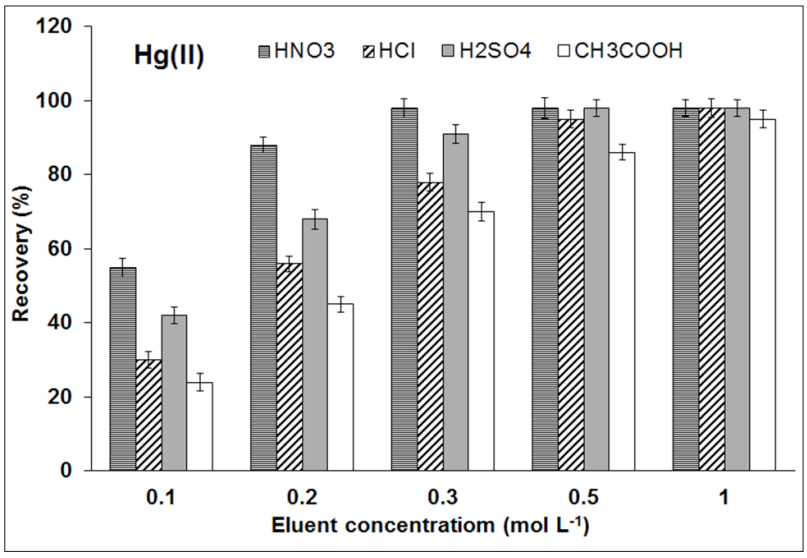

Fig. 6. Recovery percentage in presence of different acids

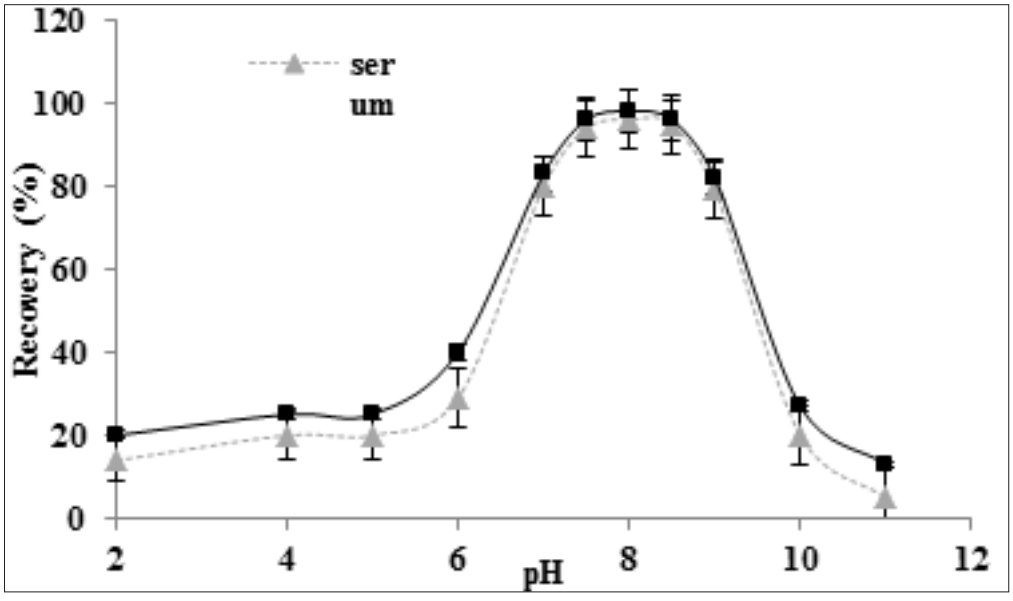

Fig.7. The effect of pH on mercury extraction by MOF

human body and caused different acute disease. In proposed conditions, the recovery of Hg extraction was obtained 25% and 97.6% by IL and MOF/IL, respectively at pH=8. The mechanism of mercury extraction of MOF/IL was mainly obtained by the electrostatic attractions of deprotonated nitrogen and carbocyclic groups (N, COO) with the positively charged mercury ions at pH=8. At acidic pH, the surface of MOF, especially charge of groups have positive (+) and similar to Hg^{2+}, so, the recovery of extraction mercury was decreased. However, in optimized pH, the MOF sorbent had negative charge and electrostatic attraction caused to extract mercury. At high pH more than 8.5, the recovery efficiencies were decreased due to the formation of hydroxyl complexes of mercury [Hg (OH)2]. Therefore, Ph=8 selected as optimized pH by USA- IL-µ-SPE procedure.

3.5.3. Effect of MOF Mass

The mass of MOF was evaluated as effective parameter for mercury absorption among 1-40 mg. Based on mass results, the optimal value was mass 20 mg for mercury absorption by the MOF. For optimization of proposed method, the amounts of $[Zn_2(bdc)_2(dabco)]_n$ in the range of 1 to 40 mg were studied for mercury extraction in serum and standard samples. The results showed us, less than 18 mg of MOF caused to decrease the extraction efficiency of mercury. So, 20 mg of $[Zn_2(bdc)_2(dabco)]_n$ was used by USA- IL-µ-SPE procedure (Fig. 8).

3.5.4. Effect of volume of serum

The optimized sample volume on the recovery of Hg(II) ions based on USA- IL-µ-SPE procedure were examined from 1 mL to 25 mL of standard and serum samples. The volume of serum was investigated as effective parameter for mercury absorption. Based on the results, the optimal value was obtained less than 18 ml for water sample by the MOF. By results, the quantitative recovery was achieved (< 95%) for 15 mL and 12 mL of standard solution and serum, respectively with concentration of 0.1 – 5.5 µg L^{-1} of mercury (CV-AAS). The recovery was decreased more than 12 mL and 15 mL for volume of serum and standard samples by proposed method. So, 10 mL of volume sample was used by USA- IL-µ-SPE method at pH=8 (Fig. 9).

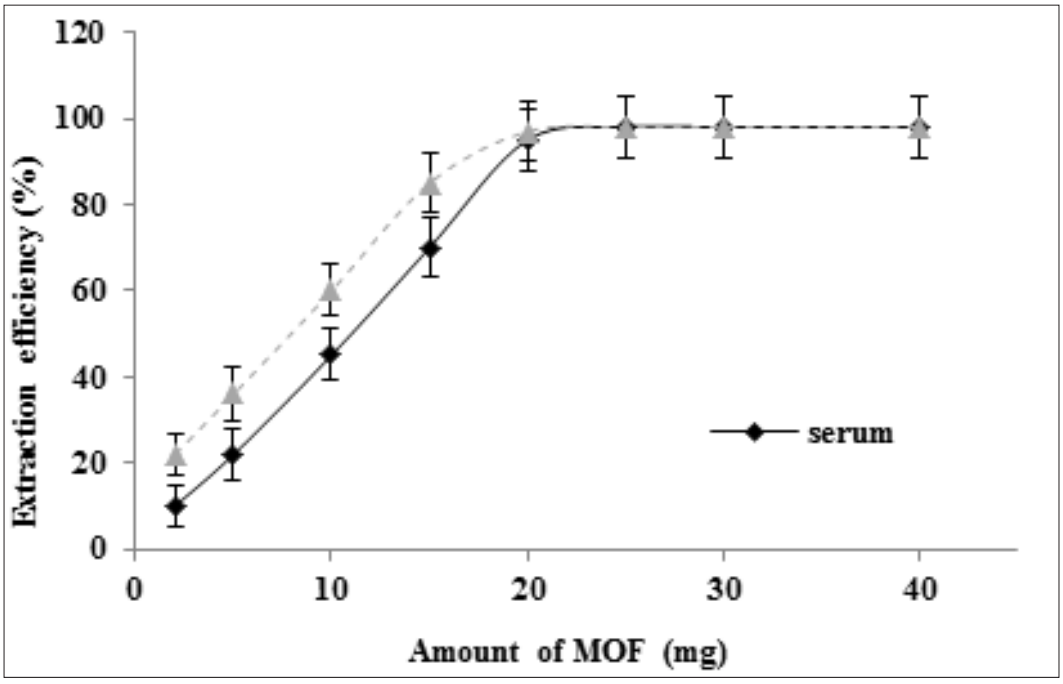

Fig. 8. The effect of MOF mass on mercury extraction

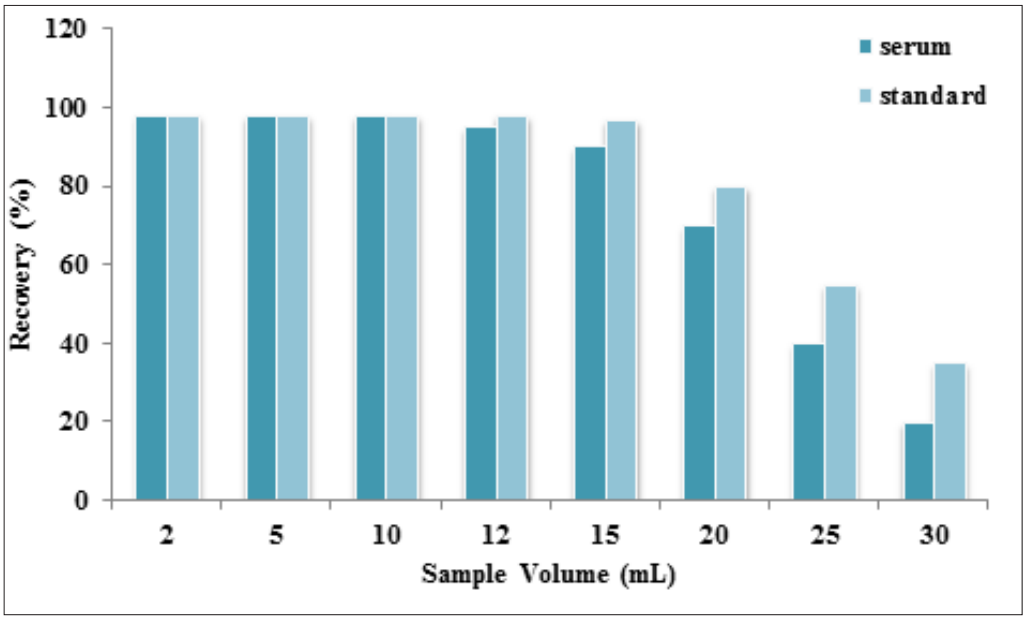

Fig. 9. The effect of sample volume on mercury extraction

3.5.5. Effect of ILs for mercury extraction

The IL was investigated as effective parameter for mercury absorption between 5-100 mg, and the optimized result was selected 50 mg. A hydrophobic ionic liquids such as; [MMIM] [PF_6], [HMIM] [PF_6] and [OMIM][PF_6] as a green solvent was used to separate MOF from the serum and standard solution (Fig. 10). The different amount of IL (5-100 mg) for separation of $[Zn_2(bdc)_2(dabco)]_n$ from serum phase were used and examined. The results showed us, the good recovery was achieved with 65 mg of [HMIM][PF_6] and 45 mg of [OMIM][PF_6]. Therefore, 50 mg of [OMIM][PF_6] was selected by proposed method. In addition, the effect of [OMIM][PF6] for extraction of mercury in serum matrix was investigated without $[Zn_2(bdc)_2(dabco)]_n$ sorbents. The results showed us, the extraction recoveries of Hg were obtained about 12 % by $[Zn_2(bdc)_2(dabco)]_n$ which was depended to amino acid complexation in serum.

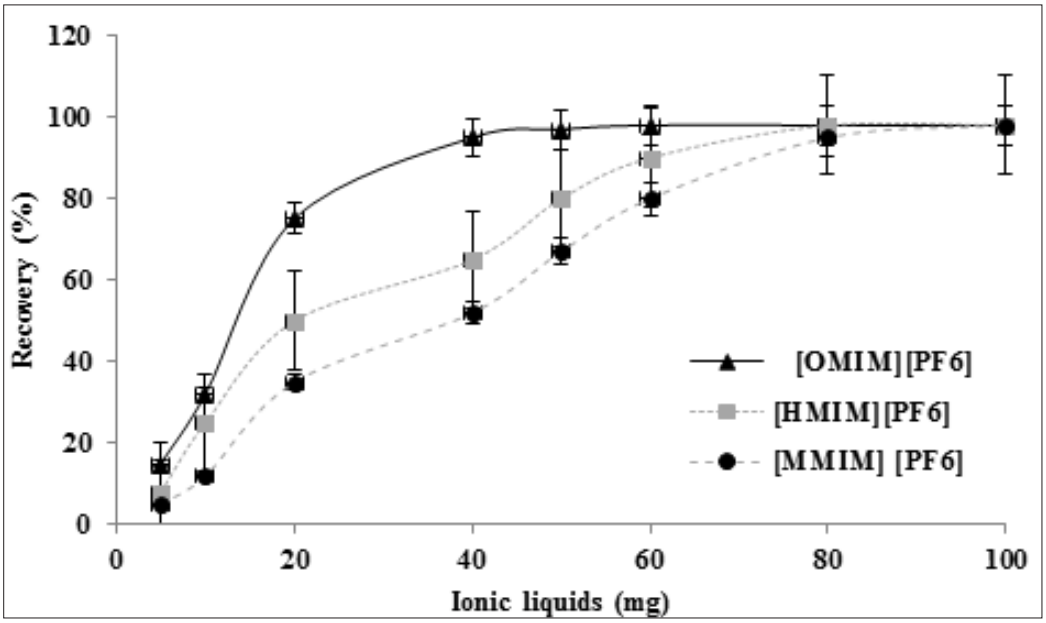

Fig. 10. The effect of different ionic liquids on mercury extraction

Table 2. The interference of some coexisting ions in serum samples on the recovery of mercury ions under the optimal condition.

Ions	Concentration ratio ($C_{interferent\ ion}/C_{Hg^{2+}}$)		Mean of Recovery (%)	
	Standard	Serum	Standard	Serum
Cr^{3+}, Co^{2+}, Pb^{2+}, V^{3+}, Mn^{2+}	500	400	96.4	95.9
I^-, Br^-, F^-, NO_3^-,	750	620	98.6	96.2
Na^+, K^+, Cl^-,Ca^{2+}, Mg^{2+}	1400	1100	97.7	95.1
Ni^{2+}, Ag^+, Cd^{2+}	35	20	99.3	97.5
Zn^{2+}, Cu^{2+}	120	100	97.0	96.8

3.5.6. Adsorption capacity

The important factor for analyzing of mercury with $[Zn_2(bdc)_2(dabco)]_n$ as MOF sorbent was adsorption capacity factor (ACF). In batch system, the ACF of Hg (II) was studied for 10 mL of human serum and standard solution at pH=8. The ACF of MOF for mercury vapor in GC closed glass was 149.56 mg g^{-1}. Based on characteristics of $[Zn_2(bdc)_2(dabco)]_n$ the most ACF related to chemical bounding of MOF as compared to physical adsorption by MOF. So, $[Zn_2(bdc)_2(dabco)]_n$ with high ACF was considered as excellent MOF sorbent for extraction of Hg (II) from serum and standard solution samples.

3.6. Interference Study

By USA-IL-μ-SPE procedure based on MOF for real samples, the interference of some coexisting ions encountered in serum samples on the recovery of Hg (II) ions was investigated under the optimal condition. This procedure was performed by adding various amounts of the interfering ions to 10 mL of standard sample solution containing 5.5 μg L^{-1} of Hg (II). Taking as criterion for interference the deviation of the recovery more than ±5%, the obtained results (Table 2) showed that most of the probable concomitant cations and anions had no considerable effect on the recovery efficiencies of Hg (II) ions under the selected conditions.

3.7. Validation of results

The mercury absorption capacity was examined among different applications of MOF as hybrid inorganic-organic nanoporous materials by USA-IL-μ-SPE method. The intra-day analysis of mercury was shown in Table 3 and based on this result; MOF is good candidate for mercury adsorption.

The USA-IL-μ-SPE method was used for ultra-trace mercury determination in standard solution and serum samples. The results based on average of three determinations, for Hg (II) were achieved in serum samples. For validation of results, real samples in serum and standard solution was verified by spiking of mercury standard concentration (Tables 4). The favorate recovery showed that the proposed method had good accuracy in serum matrix. The recoveries of spiked samples for serum and standard solution were obtained more than 95%. The developed method based on MOF /IL was satisfactory demonstrated for mercury analysis in serum. The concentration of Hg in petroleum (subject) and office worker (control) were studied by USA-IL-μ-SPE procedure (N=-50). There were no significant differences between

Table 3. The intra-day analysis of mercury with MOF by USA-IL-μ-SPE method

Parameter (Intra-day)	Serum sample	Standard sample
PF[a]	9.8	10.2
LOD[b] (n=10, ng L^{-1})	6.5	6.8
RSD[c] (n=6, %)	4.2	3.3
Linear range ($\mu g\ L^{-1}$)	0.02 – 5.5	0.02 – 6.0
Correlation coefficient	0.9988	0.9992

[a] Preconcentration factor, [b] Limit of detection, [c] Relative standard deviation.

Table 4. Validation of USA-IL-μ-SPE method based on MOF/IL by spiking of mercury standard concentration in real samples (μg L^{-1})

Sample	Added	Found[a]	Recovery (%)
	Hg (II)	Hg(II)	Hg(II)
Serum	-----	0.48 ± 0.02	-----
	0.5	0.97 ± 0.05	98
	1.0	1.51 ± 0.07	103
Serum	-----	2.55 ± 0.13	-----
	1.0	3.52 ± 0.12	97
	2.0	4.48 ± 0.23	96.5
Water	-----	3.11± 0.14	-----
	1.0	4.07 ± 0.21	96
	2.0	5.14 ± 0.27	102
Water	-----	0.26 ± 0.01	-----
	0.2	0.47 ± 0.02	105
	0.4	0.65 ± 0.02	97.5

[a] Mean of three determinations±confidence interval (P= 0.95, n=5)

exposed subjects and unexposed controls in terms of age and sex. The mean concentration of mercury in control groups was obtained under 1.0 μg L^{-1}. In addition, for validation of methodology, standard reference material (SRM 1641e) for inorganic mercury was analyzed by MOF/IL. Table 5 was approved the validation of developed USA-IL-μ-SPE method. The Ethical Committee of Tehran Medical Sciences, Islamic Azad University, approved the blood sampling guidance in the human body based on the Helsinki rules (E.C.: IR.IAU.PS.REC.1398.272).

4. Conclusions

In this study, $Zn_2(BDC)_2(DABCO)$ MOF was synthesized by solvothermal method at 90 °C for 3 h via the self-assembly metal centers and linkers using DMF solvent. Based on the results, the MOF was propped as a good candidate for mercury absorption. The highest mercury absorption was observed in pH=8, mass of MOF 20 mg, volume of serum 10 ml, volume of water 15 ml, and IL optimized 50 mg in presence of HNO_3 as optimized acid. Also, the interference of concomitant cations and anions had no considerable effect on the recovery efficiencies of Hg (II) ions under the selected conditions. Therefore, these properties can be resulted to many advantages in the future to absorb of hazardous materials.

5. References

[1] N. Motakef-Kazemi, S.A. Shojaosadati, A. Morsali, Evaluation of the effect of nanoporous nanorods

Table 5. Validation of developed USA- IL-μ-SPE method based on MOF with standard reference material (SRM)

Sample	Certified (μg L^{-1})	Added (μg L^{-1})	Found [a] (μg L^{-1})	Recovery (%)
			Hg (II)	
SRM 1641e [b]	1.016 ± 0.017	---	0.952 ± 0.048	----
		0.5	1.446 ± 0.087	98.8
		1.0	1.921 ± 0.126	96.9
SRM 3668[c]	0.910 ± 0.055	---	0.897 ± 0.052	----
		0.5	1.380 ± 0.092	96.6
		1.0	1.875 ± 0.103	97.8

[a] Mean of three determinations ± confidence interval (P = 0.95, n =5).

[b] NIST, SRM 1641e, total mercury in water (p=0.95).

c Mercury in Frozen Human Urine

$Zn_2(bdc)_2(dabco)$ dimension on ibuprofen loading and release, J. Iran. Chem. Soc. 13 (2016) 1205–1212.

[2] S. Hajiashrafi, N. Motakef Kazemi, Preparation and evaluation of ZnO nanoparticles by thermal decomposition of MOF-5, Heliyon 5 (2019) e02152.

[3] N. Motakef-Kazemi, S.A. Shojaosadati, A. Morsali, In situ synthesis of a drug-loaded MOF at room temperature, Micropor. Mesopor. Mat. 186 (2014) 73–79.

[4] B. Miri, N. Motakef-Kazemi, S.A. Shojaosadati, A. Morsali, Application of a nanoporous metal organic framework based on iron carboxylate as drug delivery system, Iran. J. Pharm. Res. 17(4) (2018) 1164-1171.

[5] S.I. Noro, S. Kitagawa, M. Kondo, K. Seki, A new methane adsorbent, porous coordination polymer, Angew Chem. Int. Ed. 39 (2000) 2082–2084.

[6] K.S. Min, Self-assembly and selective guest binding of three-dimensional open-frame work solids from a macrocyclic complex as a trifunctional metal building block, Chem. Eur. J. 7 (2001) 303–313.

[7] M. Fujita, Y.J. Kwon, S. Washizu, K. Ogura, Preparation, clathration ability, and catalysis of a two-dimensional square network material composed of cadmium(II) and 4,4'-bipyridine, J. Am. Chem. Soc. 116 (1994) 1151–1152.

[8] O.R. Evans, W. Lin, Crystal engineering of NLO materials based on metal−organic coordination networks, Acc. Chem. Res. 35 (2002) 511–522.

[9] O.R. Evans, W. Lin, Crystal engineering of nonlinear optical materials based on interpenetrated diamondoid coordination networks, Chem. Mater. 13 (2001) 2705–2712.

[10] M. Oh, C.A. Mirkin, Ion exchange as a way of controlling the chemical compositions of nano- and microparticles made from infinite coordination polymers, Angew Chem. Int. Ed. 45 (2006) 5492–5494.

[11] R. Kitaura, S. Kitagawa, Y. Kubota, T.C. Kobayashi, K. Kindo, Y. Mita, A. Matsuo, M. Kobayashi, H. Chang, T.C. Ozawa, M. Suzuki, M. Sakata, M. Takata, Formation of a one-dimensional array of oxygen in a microporous metal-organic solid, Sci. 298 (2002) 2358–2361.

[12] P. Horcajada, T. Chalati, C. Serre, B. Gillet, C. Sebrie, T. Baati, J.F. Eubank, D. Heurtaux, P. Clayette, C. Kreuz, J.S. Chang, Y.K. Hwang, V. Marsaud, P.N. Bories, L. Cynober, S. Gil, G. Ferey, P. Couvreur, R. Gref, Porous metal-organic-framework nanoscale carriers as a potential platform for drug delivery and imaging, Nat. Mater. 9 (2010) 172–178.

[13] B. Chen, L. Wang, F. Zapata, G. Qian, A luminescent microporous metal−organic framework for the recognition and sensing of anions, J. Am. Chem. Soc. 130 (2008) 6718–6719.

[14] A.J. Fletcher, K.M. Thomas, M.J. Rosseinsky, Flexibility in metal-organic framework materials: impact on sorption properties, J. Solid State Chem. 178 (2005) 2491–2510.

[15] M.D. Allendorf, C.A. Bauer, R.K. Bhakta, R.J.T. Houk, Luminescent metal–organic frameworks, Chem. Soc. Rev. 38 (2009) 1330-1352.

[16] S.M. Humphrey, T.J. Angliss, M. Aransay, D. Cave, L.A. Gerrard, G.F. Weldon, P.T. Wood, Bimetallic metal-organic frameworks containing the $[M2,x\text{-}pdc)_2^{-2}]$(M = Cu, Pd, Pt; x = 4, 5) building block–synthesis, structure, and magnetic properties, Z. Anorg. Allg. Chem. 633 (2007) 2342-2353.

[17] C.G. Silva, A. Corma, H. García, Metal–organic frameworks as semiconductors. J. Mater. Chem. 20 (2010) 3141-3156.

[18] M. Hunsom, K. Pruksathorn, S. Damronglerd, H. Vergnes, P. Duverneuil, Electrochemical treatment of heavy metals (Cu^{2+}, Cr^{6+}, Ni^{2+}) from industrial effluent and modeling of copper reduction, Water Res. 39 (2005) 610-616.

[19] A. El-Samrani, B. Lartiges, F. Villiéras, Chemical coagulation of combined sewer overflow: heavy metal removal and treatment optimization. Water Res. 42 (2008) 951-960.

[20] H. Ozaki, K. Sharma, W. Saktaywin, Performance of an ultra-low-pressure reverse osmosis membrane (ULPROM) for separating heavy metal: effects of interference parameters, Desalination 144 (2002) 287-294.

[21] Z. Wang, J. Xu, Y. Hu, H. Zhao, H. Zhou, Y. Liu, Z. Lou, X. Xu, Functional nanomaterials: Study on aqueous Hg(II) adsorption by magnetic Fe_3O_4@ SiO_2-SH nanoparticles, J. Taiwan Inst. Chem. Eng. 60 (2016) 394-402.

[22] L. Rahmanzadeh, M. Ghorbani, M. Jahanshahi, Effective removal of hexavalent mercury from aqueous solution by modified polymeric nanoadsorbent, J. Water Environ. Nanotechnol. 1

(2016) 1-8.

[23] K. Yaghmaeian, R. Khosravi Mashizi, S. Nasseri, A.H. Mahvi, M. Alimohammadi, S. Nazmara, Removal of inorganic mercury from aquatic environments by multi walled carbon nanotubes, J. Environ. Health Sci. Eng. 13 (2015) 55.

[24] Q.D. Qin, J. Ma, K. Liu, Adsorption of nitrobenzene from aqueous solution by MCM-41, J. Colloid Interface Sci. 315 (2007) 80–86.

[25] L. Xie, D. Liu, H. Huang, Q. Yang, C. Zhong, Efficient capture of nitrobenzene from waste water using metal–organic frameworks, Chem. Eng. J. 246 (2014) 142–149.

[26] D.V. Patil, P.B. Somayajulu Rallapalli, G.P. Dangi, R.J. R.S. Tayade, Somani, H.C. Bajaj, MIL-53(Al): An efficient adsorbent for the removal of nitrobenzene from aqueous solutions, Ind. Eng. Chem. Res. 50 (2011) 10516–10524.

[27] N. T. Abdel-Ghani, G. A. El-Chaghaby, F. S. Helal, Individual and competitive adsorption of phenol and nickel onto multiwalled carbon nanotubes, J. Adv. Res. 6 (2015) 405-415.

[28] Z. Zhaoa, X. Li, Z. Li, Adsorption equilibrium and kinetics of p-xylene on chromium-based metal organic framework MIL-101, Chem. Eng. J. 173 (2011) 150–157.

[29] A.A. Adeyemo, I.O. Adeoye, O.S. Bello, Metal organic frameworks as adsorbents for dye adsorption: overview, prospects and future challenges, Toxicol. Environ. Chem. 94(10) (2012) 1846–1863.

[30] M.M. Tong, D.H. Liu, Q.Y. Yang, S. Devautour-Vinot, G. Maurin, C.L. Zhong, Influence of framework metal ions on the dye capture behavior of MIL-100 (Fe, Cr) MOF type solids, J. Mater. Chem. A 1 (2013) 8534–8537.

[31] M.A. Al-Ghouti, M.A.M. Khraisheh, S.J. Allen, M.N. Ahmad, The removal of dyes from textile wastewater: a study of the physical characteristics and adsorption mechanisms of diatomaceous earth, J. Environ. Manage. 69 (2003) 229–238.

[32] J. Galán, A. Rodríguez, J.M. Gómez, S.J. Allen, G.M. Walker, Reactive dye adsorption onto a novel mesoporous carbon, Chem. Eng. J. 219 (2013) 62–68.

[33] A. Sayari, S. Hamoudi, Y. Yang, Applications of pore-expanded mesoporous silica: removal of heavy metal cations and organic pollutants from wastewater, Chem. Mater. 17 (2005) 212-216.

[34] S. Babel, T.A. Kurniawan, Low-cost adsorbents for heavy metals uptake from contaminated water: a review, J. Hazard. Mater. B97 (2003) 219–243.

[45] L. Rasuli, A.H. Mahvi, Removal of humic acid from aqueous solution using MgO nanoparticles, J. Water Chem. Tech. 38(1) (2016) 21–27.

[36] M.R. Mehmandoust, N. Motakef-Kazemi, F. Ashouri, Nitrate adsorption from aqueous solution by metal–organic framework MOF-5, Iran. J. Sci. Technol. Trans. A-Science. 43(2) (2019) 443–449.

[37] A. Bhatnagara, E. Kumarb, M. Sillanpää, Nitrate removal from water by nano-alumina: Characterization and sorption studies, Chem. Eng. J. 163 (2010) 317–323.

[38] J.D. Park, W. Zheng, Human exposure and health effects of inorganic and elemental mercury, J. Prev. Med. Public Health 45 (2012) 344–352.

[39] M.A. Bradley, B.D. Barst, N. Basu, A review of mercury bioavailability in humans and fish, Int. J. Environ. Res. Public Health 14 (2017) 169.

[40] B.F. Azevedo, L.B. Furieri, F.M. Pecanha, G.A. Wiggers, P.F. Vassallo, M.R. Simoes, J. Fiorim, P.R. Batista, M. Fioresi, L. Rossoni, I. Stefanon, M.J. Alonso, M. Salaices, D.V. Vassallo, Toxic effects of mercury on the cardiovascular and central nervous systems, J. Biomed. Biotechnol. 2012 (2012) 1-11.

[41] K.M. Rice, E.M. Walker Jr, M. Wu, C. Gillette, E.R. Blough, Environmental mercury and its toxic effects, J. Prev. Med. Public Health 47 (2014) 74–83.

[42] S.E. Orr, C.C. Bridges, Chronic kidney disease and exposure to nephrotoxic metals, Int. J. Mol. Sci. 18 (2017) 1039.

[43] E. Afshar, H. Mohammadi-Manesh, H. Dashti Khavidaki, Removal of Hg (I) and Hg (II) ions from aqueous solutions, using TiO_2 nanoparticles, Pollution. 3 (2017) 505-516.

[44] K. Suresh Kumar Reddy, B. Rubahamya, A. Al Shoaibi, C. Srinivasakannan, Solid support ionic liquid (SSIL) adsorbents for mercury removal from natural gas, Int. J. Environ. Sci. Technol. 16 (2019) 1103–1110.